24. Pachnis, V., Mankoo, B. & Costantini, F. *Development* **119,** 1005–1017 (1993).
25. Sainio, K. *et al. Int. J. dev. Biol.* **38,** 77–84 (1994).
26. Trupp, M. *et al. J. Cell Biol.* **130,** 137–148 (1995).
27. Hemmati Brivanlou, A., Kelly, O. G. & Melton, D. A. *Cell* **77,** 283–295 (1994).
28. Takahashi, M. *et al. Oncogene* **8,** 2925–2929 (1993).
29. Rathjen, F. & Schachner, M. *EMBO J.* **3,** 1–10 (1984).
30. Nieuwkoop, P. D. & Faber, J. *Normal Table of Xenopus laevis (Daudin)* (North-Holland, Amsterdam, 1975).

ACKNOWLEDGEMENTS. We thank M. Umbhauer, M. Jones, J. Smith, A. Snape, S. Ley, G. Panayotou, N. Lamarche and C. Ibanez for advice, discussions and encouragement; D. Wilkinson for the Sek-1 cDNA clone; W. Hatton for histology; and J. Smith, R. Krumlauf and D. Wilkinson for comments on the manuscript. This work was supported by the MRC and a grant from the NIH to V.P. and F.C. P.D. was supported by a European Union postdoctoral fellowship.

CORRESPONDENCE and requests for materials should be addressed to V.P. (e-mail: v-pachni@nimr.mrc.ac.uk).

Synaptic strengthening through activation of Ca^{2+}-permeable AMPA receptors

J. G. Gu, C. Albuquerque, C. J. Lee & A. B. MacDermott

Department of Physiology and Cellular Biophysics and the Center for Neurobiology and Behavior, Columbia University, 630 W. 168th Street, New York, New York 10032, USA

Postsynaptic Ca^{2+} elevation during synaptic transmission is an important trigger for short- and long-term changes in synaptic strength in the vertebrate central nervous system[1]. The AMPA (α-amino-3-hydroxy-5-methyl-4-isoxazoleproprionate) receptors, a subfamily of glutamate receptors, mediate much of the excitatory synaptic transmission in the brain and spinal cord[2]. It has been shown that a subtype of the AMPA receptor is Ca^{2+}-permeable[3–6] and is present in subpopulations of neurons[7–12]. When synaptically localized[13], these receptors should mediate postsynaptic Ca^{2+} influx, providing a trigger for changes in synaptic strength. Here we show that Ca^{2+}-permeable AMPA receptors are synaptically localized on a subpopulation of dorsal horn neurons, that they provide a synaptically gated route of Ca^{2+} entry, and that activation of these receptors strengthens synaptic transmission mediated by AMPA receptors. This pathway for postsynaptic Ca^{2+} influx may provide a new form of activity-dependent modulation of synaptic strength.

Fast application of a hyperosmotic solution to dorsal horn neurons in culture caused a large increase in the probability of transmitter release, as indicated by an enhancement in the frequency of miniature excitatory postsynaptic currents (mEPSCs; Fig. 1*a*) and shown previously at several types of synapses[14–17]. The mEPSCs in our studies were mediated by AMPA receptors because they were blocked by 25 μM CNQX (6-cyano-7-nitroquinoxaline-2,3-dione) (Fig. 1*a*). The enhanced release of neurotransmitter was retained in a low-Ca^{2+} hyperosmotic bath (Fig. 1*a*). Synaptic Ca^{2+} transients were evoked by hyperosmotic solution in the presence of 25 μM D-APV (D-2-amino-5-phosphonovaleric acid) and were blocked by 25 μM CNQX (Fig. 1*b*), indicating that they were due to Ca^{2+} entry through synaptically gated Ca^{2+}-permeable AMPA receptors. The Ca^{2+} transients required Ca^{2+} influx and were not due solely to release of Ca^{2+} from intracellular stores[18], because a hyperosmotic bath with no added Ca^{2+} did not evoke Ca^{2+} transients (Fig. 1*b*). These results demonstrate the synaptic localization of Ca^{2+}-permeable AMPA receptors on dorsal horn neurons in culture and show that their activation leads to an increase in postsynaptic intracellular calcium ion concentration ($[Ca^{2+}]_i$) in neurites.

JSTX-3, a synthetic derivative from the venom of the spider *Nephila clavata*[19], selectively inhibits recombinant AMPA receptors lacking the GluR2 subunit[20], a molecular determinant whose absence is required for Ca^{2+} permeability of the AMPA receptors[4–6]. We tested the ability of the use-dependent JSTX-3 (ref. 20) to select among natively expressed AMPA receptors on neurons that express different combinations of Ca^{2+}-permeable and Ca^{2+}-impermeable AMPA receptors[21]. The relative level of expression of Ca^{2+}-permeable AMPA receptors was determined by the

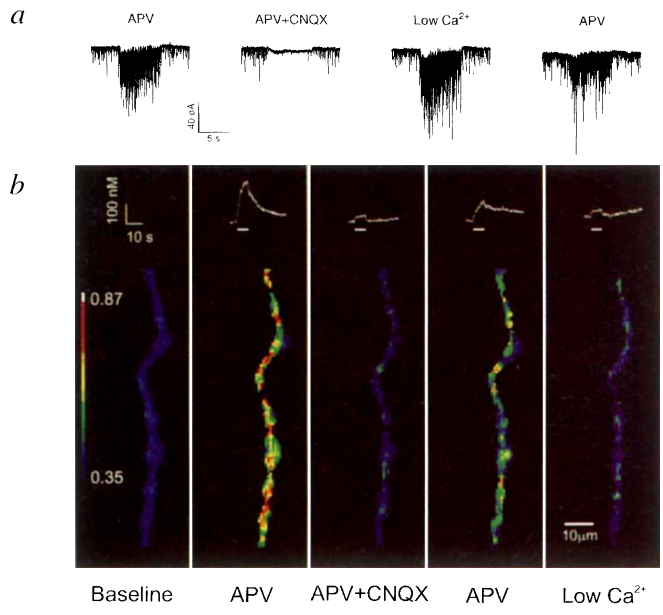

FIG. 1 Hyperosmotic solution transiently promotes transmitter release in a Ca^{2+}-independent manner (*a*), enhancing Ca^{2+} influx through postsynaptic Ca^{2+}-permeable AMPA receptors (*b*); *a* and *b* were recorded from different cells. At least 2 min were allowed between applications to permit replenishing of the synaptic vesicle pool. *a*, CNQX quickly and effectively blocked mEPSCs when applied with hyperosmotic solution, which enhanced mEPSC frequency even in low external $[Ca^{2+}]$. *b*, Fura-2 ratio images of a neurite to which hyperosmotic solution was applied in the presence of the indicated drugs. Insets, traces of $[Ca^{2+}]_i$ against time for each of the conditions represented by the images. Bars under the traces represent the application time of the hyperosmotic solutions. The artefact present in all traces may be due to optical perturbation, caused by application of the hyperosmotic solution. Minimum and maximum ratios in the colour scale correspond, respectively, to 1 nM and 450 nM Ca^{2+}. The baseline $[Ca^{2+}]_i$ increased from 50–70 nM between the first and last application of hyperosmotic solution. The average change in $[Ca^{2+}]_i$ evoked by hyperosmotic solution with D-APV when measured over a large section of neurite was 95 ± 79 nM ($n = 3$). This Ca^{2+} elevation was blocked by 95 ± 8% by 25 μM CNQX. In a similar series of experiments using hyperosmotic solution with 75 mM $CaCl_2$ and D-APV, the change in $[Ca^{2+}]_i$ was 28 ± 20 nM, which was inhibited 86 + 13% by CNQX ($n = 3$).

METHODS. Spinal-cord dorsal-horn neuron cultures were prepared as described[10] and used between 2–5 weeks. Cells were perfused with bath solution containing (in mM) 145 NaCl, 5 KCl, 2 $CaCl_2$, 2 $MgCl_2$, 10 HEPES, 5.5 D-glucose and 5×10^{-4} tetrodotoxin (TTX) (pH 7.3, 325 mOsm, at room temperature). Hyperosmotic solution was bath solution with osmolarity adjusted to 530 mOsm with sucrose, plus 30 μM $LaCl_3$ to block all voltage-gated Ca^{2+} channels[10], plus 3 mM $CaCl_2$ (5 mM $CaCl_2$ total) and 25 μM D-APV. Low-Ca^{2+} hyperosmotic solution did not have $CaCl_2$ or D-APV. Test and wash solutions were applied through a fast perfusion system. For *a*, neurons were patch-clamped at −70 mV in perforated patch configuration using Cs^+-filled electrodes[26]. For *b*, neurons were loaded with 1 mM Fura-2 pentapotassium salt[27] through a potassium gluconate patch pipette in the whole-cell configuration. After 10 min of dye loading, the pipette was withdrawn and the dye allowed to diffuse into the neurites for an additional 20 min. Background-subtracted ratio images were obtained by the single-wavelength ratio method[28], using 340 or 360 nm as the reference wavelength and 380 nm as the measured wavelength. Each panel in *b* is 1 image frame taken at the peak of the response, with an average baseline subtracted for each condition.

apparent reversal potential (E_{rev}) of currents evoked by 100 μM kainate in a Na^+-free both with 10 mM Ca^{2+} (0 Na^+/10 Ca^{2+} bath)[21] (Fig. 2 legend). Figure 2*a* shows data from a cell expressing large numbers of Ca^{2+}-permeable AMPA receptors, as indicated by an E_{rev} near −40 mV. The amplitude of the kainate-evoked current was strongly decreased, with little change in E_{rev}, when neurons were treated with 1 μM JSTX-3 plus 100 μM kainate. The currents were almost completely blocked by subsequent exposure to 2 μM JSTX-3 plus kainate. Figure 2*b* shows data from a cell expressing few Ca^{2+}-permeable AMPA receptors, as indicated by an E_{rev} near −90 mV. Little block was evident following 1 μM ($n = 3$; not shown) or 10 μM ($n = 4$) JSTX-3 except for a slight negative shift in the E_{rev}. Figure 2*c* shows data from a cell expressing a mixture of both Ca^{2+}-permeable and Ca^{2+}-impermeable AMPA receptors (E_{rev} near −60mV). JSTX-3 shifted the E_{rev} to a more negative value and decreased current amplitude, presumably by decreasing the contribution of the Ca^{2+}-permeable channels to the total AMPA receptor population. These results show that E_{rev} in a 0 Na^+/10 Ca^{2+} bath is a good indicator of the relative proportion of Ca^{2+}-permeable AMPA receptor expressed on each cell and that JSTX-3 block is selective for native Ca^{2+}-permeable AMPA receptors.

If Ca^{2+}-permeable AMPA receptors participate in synaptic transmission, the amplitudes of mEPSCs should decrease in the presence of JSTX-3. The data shown in Fig. 3*A* were recorded from a cell expressing moderate numbers of Ca^{2+}-permeable

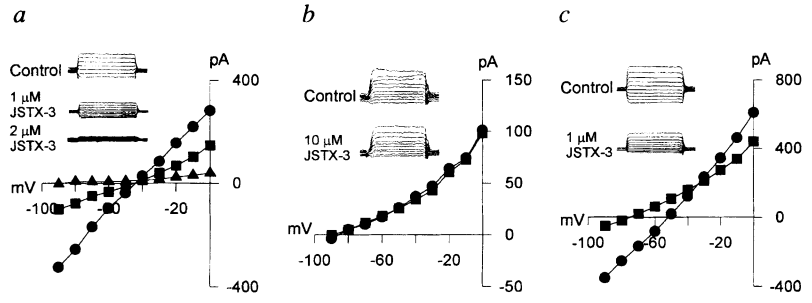

FIG. 2 JSTX-3 block is selective for native Ca^{2+}-permeable AMPA receptors. Currents were evoked by 100 μM kainate in a 0 Na^+/10 Ca^{2+} bath at different membrane potentials[21] before and after exposure to JSTX-3. Insets show raw traces of the currents from which the corresponding *I–V* curves are constructed. *a*, Data from a neuron expressing high numbers of Ca^{2+}-permeable AMPA receptors. The amplitudes of kainate-evoked currents are plotted before (●) and after block with 1 μM (■), or 2 μM JSTX-3 (▲). For all cells of this group with an E_{rev} near −40 mV (−39.3 ± 5.1 mV; $n = 3$, mean ± s.d.), the apparent Ca^{2+} permeability, $P_{Ca^{2+}}/P_{Cs^+}$ (ref. 22) was 1.14 ± 0.28. The kainate-evoked current was decreased by ~70% (71.3% ± 11.5%) by 1 μM JSTX-3, with no change in E_{rev}. *b*, 10 μM JSTX-3 has no effect on Ca^{2+}-impermeable AMPA receptors, as can be seen by comparing kainate-evoked current amplitudes under control conditions (●) and after addition of 10 μM JSTX-3 (■). For cells of this group with an E_{rev} near −90 mV (−84.3 ± 8.5 mV; $n = 7$), the $P_{Ca^{2+}}/P_{Cs^+}$ value for AMPA receptors was 0.18 ± 0.06 ($n = 7$). *c*, Effect of JSTX-3 on a cell expressing both Ca^{2+}-permeable and Ca^{2+}-impermeable AMPA receptors. Kainate-evoked currents are shown under control conditions (●) and after addition of 1 μM JSTX-3 (■). For cells of this group with an E_{rev} between −40 and −70 mV (−62.3 ± 8.1 mV; $n = 6$), $P_{Ca^{2+}}/P_{Cs^+}$ was 0.43 ± 0.14. 1 μM JSTX-3 decreased current amplitude and shifted the E_{rev} to a more negative value (−84.0 ± 20.5 mV; $n = 6$) and the $P_{Ca^{2+}}/P_{Cs^+}$ to 0.22 ± 0.15.

METHODS. Neurons were voltage-clamped at −70 mV in perforated-patch configuration with Cs^+ filled electrodes[26]. Bath solution also contained 10 μM bicuculline, 5 μM strychnine and 25 μM D-APV. 0 Na^+/10 Ca^{2+} bath was composed of (in mM): 10 $CaCl_2$, 155 NMDG (*N*-methyl-D-glucamine), 10 HEPES, 5.5 D-glucose and 5 × 10^{-4} TTX (pH 7.3, 315–325 mOsm). The 0 Na^+/10 Ca^{2+} bath was preapplied to the cell for 1 s followed by 100 μM kainate in the same bath for 2 s. Voltage steps were applied for 4 s starting from the time when 0 Na^+/10 Ca^{2+} bath was on and ending when 0 Na^+/10 Ca^{2+} bath was off. After obtaining control data, each cell was exposed to 1–10 μM JSTX-3 plus 100 μM kainate in 0 Na^+/0 Ca^{2+} (with 20 mM CsCl added) bath for 4 min. Each preparation was subsequently washed for 2 min with normal bath and a new *I–V* curve for kainate-evoked currents was determined. JSTX-3 was added with kainate because its block is use-dependent[20]. Application of 100 μM kainate in 0 Na^+/0 Ca^{2+}/20 Cs^+ bath solution without JSTX-3 produced no significant change in E_{rev} or current amplitude in the 6 cells tested. This bath condition avoided loading the cells with Ca^{2+} during kainate application but allowed JSTX-3 access to binding sites in the open channel. Kainate-evoked currents in rat dorsal horn neurons are predominantly mediated by AMPA receptors[21].

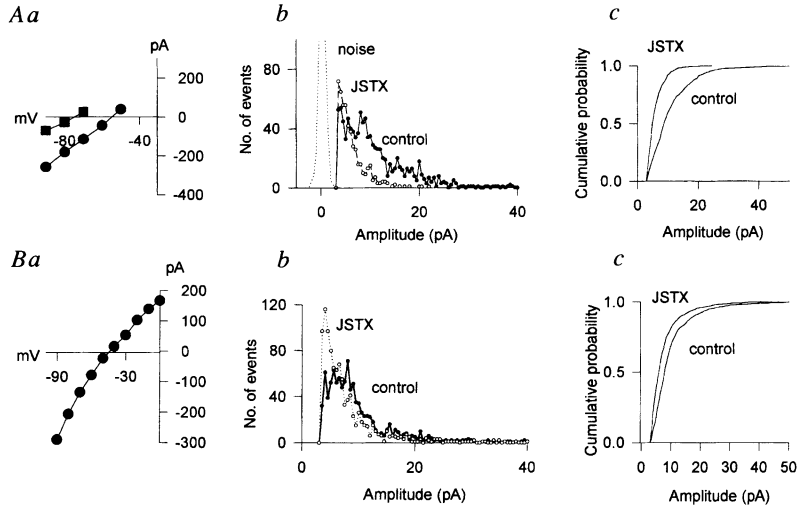

FIG. 3 Synaptic transmission through Ca^{2+}-permeable AMPA receptors is revealed by JSTX-3. *A*, *a*, The *I–V* curve is shown for kainate currents evoked in 0 Na^+/10 Ca^{2+} bath before (●) and after (■) exposure to 10 μM JSTX-3 plus 100 μM kainate for 4 min (see Methods). *b*, mEPSCs were recorded from the same cell for 5 min before (control) and after exposure to JSTX-3. Amplitudes were measured and plotted in histogram form. The noise curve shows the baseline noise amplitude measured 64 ms before each mEPSC. *c*, The same data as in *b* are plotted in a cumulative histogram. *B*, *a*, A neuron shows high expression levels of Ca^{2+}-permeable AMPA receptors as indicated by E_{rev} near −45 mV for currents evoked by 100 μM kainate in a 0 Na^+/10 Ca^{2+} bath. *b*, Amplitude histograms show mEPSCs amplitude distribution before (control) and after exposure to JSTX-3 alone. *c*, Cumulative probability amplitude histograms of 1,000 mEPSCs recorded from the same cell before and after application of JSTX-3.

METHODS. mEPSCs were recorded from neurons voltage-clamped at −70 mV in perforated patch configuration. Records were filtered at 1 kHz and sampled at 3.3 kHz. The threshold for detection of mEPSCs was set at −3 or −4 pA. Events showing summation with previous events were not included in the amplitude analysis. For 6 cells, including that in *a*, the E_{rev} was determined as for Fig. 2, before recording mEPSCs for 5 min. Cells were exposed to 10 μM JSTX-3 and 100 μM kainate in 0 Na^+/0 Ca^{2+}/20 Cs^+ bath for 4 min, washed and then 5 min of mEPSCs were recorded followed by measurement of E_{rev}. In 2 cells , JSTX-3 block was partially reversed by repeatedly stepping the membrane potential to +100 mV in the presence of 100 μM kainate for 2 s. Control applications of kainate alone in 0 Na^+/0 Ca^{2+}/20 Cs^+ bath produced no change in mEPSC amplitudes.

AMPA receptors, as indicated by a E_{rev} near −55 mV (Fig. 3*A*, *a*). mEPSCs were recorded in a normal bath for 5 min before and 5 min after a 4-min exposure to 10 μM JSTX-3 and 100 μM kainate. In this and three other cells with moderate to high levels of Ca^{2+}-permeable AMPA receptors ($E_{rev} = -49 \pm 3.9$ mV), mean mEPSC amplitude was significantly decreased from 17 ± 5 to 7.8 ± 2.4 pA by JSTX-3 ($P < 0.05$), indicating a strong contribution of Ca^{2+}-permeable AMPA receptors to the synaptic response (Fig. 3*A*, *b* and *c*). A substantial decline in mEPSC frequency was also seen after treatment with JSTX-3 (Fig. 3*A*, *b*). We attribute that, at least in part, to the reduction in some mEPSC amplitudes to a level below our threshold of detection. The mean E_{rev} in these cells following exposure to JSTX-3 plus kainate became −79 ± 2.3 mV, indicating a strong block of many of the Ca^{2+}-permeable AMPA receptors by this protocol (Fig. 3*A*, *a*). In three cells with few Ca^{2+}-permeable AMPA receptors ($E_{rev} = -95 \pm 9$ mV), JSTX-3 had no significant effect on mEPSC amplitude (8.2 ± 0.7 and 7.2 ± 1.1 pA, before and after exposure to JSTX-3, respectively). These data indicate that Ca^{2+}-permeable AMPA receptors account for more than half of the synaptically localized AMPA receptors on a subpopulation of dorsal horn neurons in culture.

Figure 3*B* shows results from an experiment in which only the synaptically released of glutamate opened AMPA receptor channels to allow use-dependent block by JSTX-3, a condition unfavourable for use-dependent block to develop but potentially less likely to produce kainate-dependent receptor modulation. After exposing a cell with high levels of Ca^{2+}-permeable AMPA receptors to JSTX-3 alone for 20 min, a clear decrease in the average mEPSC amplitude was observed (Fig. 3*B*, *b* and *c*). For cells of this group ($E_{rev} = -47 \pm 15$ mV, $n = 9$), the average mEPSC amplitude was −13.9 ± 2.4 pA before applying 10 μM JSTX-3 and was significantly decreased to 11.6 ± 2.3 pA after JSTX-3 ($P < 0.01$, paired *t*-test). For cells expressing few Ca^{2+}-permeable AMPA receptors, ($E_{rev} = -76 \pm 8, n = 6$), the average mEPSC amplitude before and after exposure to JSTX-3 was −11 ± 5.7 pA and −11 ± 6.1 pA, respectively.

NMDA receptor-dependent changes in mEPSC amplitude and frequency have yielded conflicting results in paradigms of synaptic potentiation in hippocampal neurons[16,17]. Ca^{2+} entry through voltage-gated Ca^{2+} evoked a transient enhancement of AMPA receptor function lasting for tens of minutes[22], as tested by agonist application as well as mEPSC amplitude. To test whether Ca^{2+} entry through Ca^{2+}-permeable AMPA receptors affects synaptic strength, we measured changes of mEPSC amplitudes after application of kainate to dorsal horn neurons with high or low expression levels of Ca^{2+}-permeable AMPA receptors. Figure 4*A* shows data from an experiment conducted on a neuron with high levels of Ca^{2+}-permeable AMPA receptors ($E_{rev} = -42$ mV). A significant increase in mEPSC amplitude that lasted for more than 5 min was observed after kainate application (Fig. 4*A*, *c*). The cumulative amplitude histogram (Fig. 4*A*, *b*) shows a significant shift to the right ($P < 0.01$; Kolmogorov–Smirnov test). For all cells tested expressing relatively high levels of Ca^{2+}-permeable AMPA receptors, the average mEPSC amplitude was −13.71 ± 3.93 pA at 5 min before kainate application and −18.02 ± 4.93 pA ($n = 8$) at 5 min after kainate ($P < 0.01$, paired *t*-test). When mEPSC amplitude was plotted as a function of time for these cells, a significant potentiation of mEPSC amplitude was seen over the first 5 min following kainate application (Fig. 4*A*, *c*). Two cells showed significant elevation of mEPSC amplitude for up to 15 min, the longest period tested. For the other cells, mEPSCs decayed gradually back to control. The potentiation was dependent on Ca^{2+} entry as no potentiation was observed when kainate was applied in 20 μM Ca^{2+} solution ($n = 3$), whereas subsequent kainate application in 10 mM Ca^{2+} induced potentiation (Fig. 4*C*, *a* and *b*). No consistent change in mESPC frequency was observed in these experiments.

To confirm that mEPSC potentiation is due to activation of Ca^{2+}-permeable AMPA receptors rather than to activation of voltage-gated Ca^{2+} channels caused by poor space clamp control[23] or to other effects related to kainate application, we conducted similar experiments on cells that expressed low levels of Ca^{2+}-permeable AMPA receptors (Fig. 4*B*, *a*–*c*). For all cells of this group, the average mEPSC amplitude before and 5 min after kainate applications was −9.81 ± 3.32 pA and −10.07 ± 3.03 pA

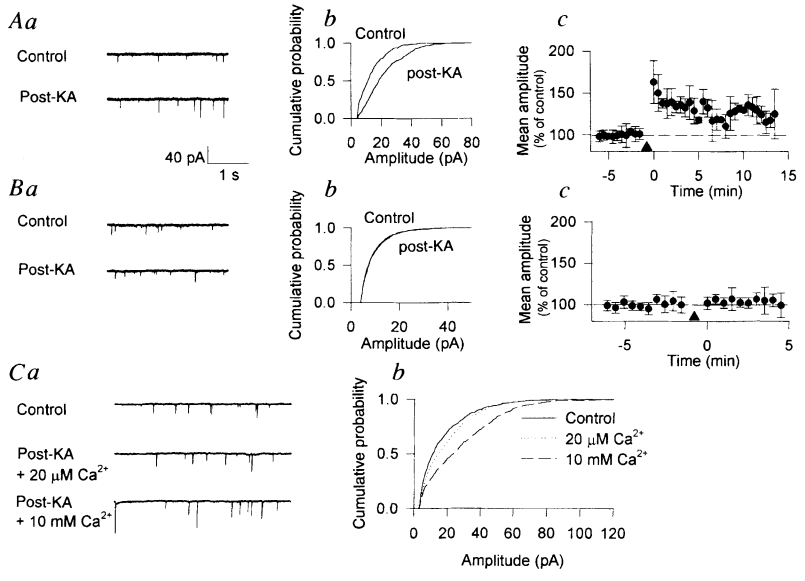

FIG. 4 mEPSC amplitude is enhanced after Ca^{2+} entry through Ca^{2+}-permeable AMPA receptors. *A*, *a*, Sample traces of mEPSCs in a cell with high expression of Ca^{2+}-permeable AMPA receptors before (top) and after (bottom) potentiation. mEPSC amplitudes were enhanced after repeated but brief activation of Ca^{2+}-permeable AMPA receptors by 1 mM kainate in the 0 Na^+/10 Ca^{2+} bath. *b*, Cumulative probability amplitude histograms of mEPSCs collected over 5 min before and 5 min after kainate pulses. Measurements are from the same cell as in *a*. *c*, Time course of potentiation by kainate from 8 cells with high expression of Ca^{2+}-permeable AMPA receptors (E_{rev} was −41.5 ± 8.2 mV; $n = 8$). mEPSC amplitude is normalized to the average mEPSC value during 5 min before kainate pulses. *B*, *a*, Sample traces from a cell with few Ca^{2+}-permeable AMPA receptors before and after kainate application using the same protocol as in *A*. *b*, Cumulative probability amplitude histograms of mEPSCs collected over 5 min before and after kainate pulses. Data are measurements from the same cell as in *a*. *c*, Normalized average amplitude of mEPSCs in 5 cells with few Ca^{2+}-permeable AMPA receptors ($E_{rev} = -70.2 \pm 6.8$ mV; $n = 5$) shows no potentiation. *C*, *a*, Sample traces of mEPSCs in a cell with high expression of Ca^{2+}-permeable AMPA receptors before (control) and after potentiation in bath with 20 μM Ca^{2+}, and bath with 10 mM Ca^{2+} as in *A*, *b* and *B*, *b*. *b*, Cumulative probability amplitude histograms of mEPSCs collected over 5 min before and after kainate pulses.

METHODS. mEPSCs were recorded as for Fig. 3. Control mEPSCs were sampled in standard bath solution for at least 5 min. 1 mM kainate was then applied 10 times to the whole cell in a 0 Na^+/10 Ca^{2+} bath solution for 0.5-s at 10-s intervals. The cell was quickly returned to standard bath solution and mEPSCs were sampled again for over 15 min. The bath conditions for kainate application were chosen to optimize Ca^{2+} entry through AMPA receptors while minimizing possible activation of voltage-gated Ca^{2+} channels that could occur as a result of voltage escape[26]. E_{rev} was determined at the end of the experiment.

($n = 5$), respectively (not significant; $P = 0.19$, paired t-test). This strongly suggests that the synaptic potentiation in Fig. 4*A*, *C* was a result of Ca^{2+} entry through Ca^{2+}-permeable AMPA receptors.

One of the most prominent distinctions between Ca^{2+}-permeable AMPA receptors and the more well known Ca^{2+}-permeable glutamate receptors, the NMDA receptors, is that the latter are subject to a voltage-dependent block by Mg^{2+}, whereas Ca^{2+}-permeable AMPA receptors are not. Consequently, the synaptic Ca^{2+} fluxes associated with activation of Ca^{2+}-permeable AMPA receptors will be prominent at negative membrane potentials where the driving force on Ca^{2+} is high[24], whereas depolarized membrane potentials will favour strong Ca^{2+} fluxes through NMDA receptors[24,25]. Thus synaptic Ca^{2+}-permeable AMPA receptors may be expected to affect synaptic strength with a different sensitivity to activity than NMDA receptors. The synaptic strengthening that occurs following Ca^{2+} entry through Ca^{2+}-permeable AMPA receptors suggests that these channels are likely to provide an important physiological signal for triggering changes in synaptic transmission. □

Received 26 February; accepted 24 April 1996.

1. Bliss, T. V. P. & Collingridge, G. L. *Nature* **361,** 31–39 (1993).
2. Jonas, P. & Spruston, N. *Curr. Opin. Neurobiol.* **4,** 366–372 (1994).
3. Iino, M., Ozawa, S. & Tsuzuki, K. *J. Physiol.* **424,** 151–165 (1990).
4. Hollmann, M., Hartley, M. & Heinemann, S. *Science* **252,** 851–853 (1991).
5. Burnashev, N., Monyer, H., Seeburg, P. H. & Sakmann, B. *Neuron* **8,** 189–198 (1992).
6. Jonas, P. & Burnashev, N. *Neuron* **15,** 987–990 (1995).
7. Jonas, P., Racca, C., Sakmann, B., Seegurg, P. H. & Monyer, H. *Neuron* **12,** 1281–1289 (1994).
8. Lerma, J., Morales, M., Ibarz, J. M. & Somohano, F. *Eur. J. Neurosci.* **6,** 1080–1088 (1994).
9. Geiger, J. R. P. *et al. Neuron* **15,** 193–204 (1995).
10. Reichling, D. B. & MacDermott, A. B. *J. Physiol.* **469,** 67–88 (1993).
11. Bochet, P. *et al. Neuron* **12,** 383–388 (1994).
12. Yin, H., Turetsky, D., Choi, D. W. & Weiss, J. H. *Neurobiol. Dis.* **1,** 43–49 (1994).
13. Otis, T. S., Raman, I. M. & Trussell, L. O. *J. Physiol.* **482,** 309–315 (1995).
14. Fatt, P. & Katz, B. *J. Physiol.* **117,** 109–128 (1952).
15. Bekkers, J. M. & Stevens, C. F. *Nature* **341,** 230–233 (1989).
16. Malgaroli, A. & Tsien, R. W. *Nature* **357,** 134–139 (1992).
17. Manabe, T., Renner, P. & Nicoll, R. A. *Nature* **355,** 50–55 (1992).
18. Murphy, T. H., Baraban, J. M. & Wier, W. G. *Neuron* **15,** 159–168 (1995).
19. Abe, T., Kawai, N. & Miwa, A. *J. Physiol.* **339,** 243–252 (1982).
20. Blaschke, M. *et al. Proc. natn. Acad. Sci. U.S.A.* **90,** 6528–6532 (1993).
21. Goldstein, P. A., Lee, C. J. & MacDermott, A. B. *J. Neurophysiol.* **73,** 2522–2534 (1995).
22. Wyllie, D. J. A., Manabe, T. & Nicoll, R. A. *Neuron* **12,** 127–138 (1994).
23. Kullmann, D. M., Perkel, D. J., Manabe, T. & Nicoll, R. A. *Neuron* **9,** 1175–1183 (1992).
24. Schneggenburger, R., Zhou, Z., Konnerth, A. & Neher, E. *Neuron* **11,** 133–143 (1993).
25. Mayer, M. L., MacDermott, A. B., Westbrook, G. L., Smith, S. J. & Barker, J. L. *J. Neurosci.* **7,** 3230–3244 (1987).
26. Kyrozis, A., Goldstein, P. A., Heath, M. J. S. & MacDermott, A. B. *J. Physiol.* **485,** 373–381 (1995).
27. Grynkiewicz, G., Poenie, M. & Tsien, R. Y. *J. biol. Chem.* **260,** 3440–3450 (1985).
28. Smith, S. J., Osses, L. R. & Augustine, G. J. in *Calcium and Ion Channel Modulation* (eds Grinnell, A. D., Armstrong, D. & Jackson, M. B.) 147–155 (Plenum, New york, 1988).

ACKNOWLEDGEMENTS. We thank O. Arancio, R. Hawkins, E. Kandel, A. Kyrozis, D. McGehee, S. Siegelbaum and G. Westbrook for comments on an earlier version of this manuscript, and M. Heath for the generous loan of his Ca^{2+}-imaging setup. A. Kyrozis and C. J. Lee developed the program for analysing miniature EPSC amplitude distribution. This work was supported by the NIH.

CORRESPONDENCE and requests for materials should be addressed to A.B.MacD. (e-mail: abm1@columbia.edu).

Transduction of bitter and sweet taste by gustducin

Gwendolyn T. Wong, Kimberley S. Gannon & Robert F. Margolskee

Department of Physiology and Biophysics, The Mount Sinai School of Medicine, One Gustave L. Levy Place, New York, New York 10029, USA

SEVERAL lines of evidence suggest that both sweet and bitter tastes are transduced via receptors coupled to heterotrimeric guanine-nucleotide-binding proteins (G proteins) (reviewed in refs 1, 2). Gustducin is a taste receptor cell (TRC)-specific G protein that is closely related to the transducins[3]. Gustducin and rod transducin, which is also expressed in TRCs (ref. 4), have been proposed to couple bitter-responsive receptors to TRC-specific phosphodiesterases to regulate intracellular cyclic nucleotides[2–5]. Here we investigate gustducin's role in taste transduction by generating and characterizing mice deficient in the gustducin α-subunit (α-gustducin). As predicted, the mutant mice showed reduced behavioural and electrophysiological responses to bitter compounds, whereas they were indistinguishable from wild-type controls in their responses to salty and sour stimuli. Unexpectedly, mutant mice also exhibited reduced behavioural and electrophysiological responses to sweet compounds. Our results suggest that gustducin is a principal mediator of both bitter and sweet signal transduction.

Gene replacement was used to generate a null mutation of the α-gustducin gene. The murine α-gustducin gene was cloned and sequences surrounding the first protein coding exon were used to create the targeting vector (Fig. 1*a*). Positive/negative selection[6] was used to enrich for embryonic stem (ES) cell clones with a homologously recombined α-gustducin allele (Fig. 1). Chimaeric mice, generated from these ES cells by blastocyst injection, were back-crossed to C57BL/6J mice. Homozygous mice harbouring the recombined gustducin allele, genetically (C57BL/6J × 129/SvEmsJ)F_2, were produced by intercrossing heterozygous animals (Fig. 1*b*). Heterozygous and homozygous null mice were viable, healthy and fertile.

Taste epithelia from homozygous null mice were morphologically indistinguishable from epithelia of wild-type littermates (Fig. 1*c–f*). Mice have three types of taste papillae: fungiform, scattered throughout the anterior two thirds of the tongue; foliate, in lateral grooves; and a single circumvallate, at the back of the tongue[7]. The null mice had all three types of taste papillae, with an appropriate number of taste buds in each papilla and a normal complement of TRCs per bud.

α-Gustducin messenger RNA is normally expressed in TRCs of circumvallate, foliate and fungiform taste papillae[3]. However, in the null mice, α-gustducin expression was not detectable in the TRCs of circumvallate (compare Fig. 1*c* and *e*), foliate or fungiform taste papillae (data not shown). The sense probe controls (Fig. 1*d,f*) showed no hybridization to lingual tissue. We conclude that the targeting event resulted in a null allele of α-gustducin.

Forty-eight-hour two-bottle preference tests[8] were used to compare the taste responses of α-gustducin null mice with those of their wild-type siblings. A preference ratio (tastant solution consumed as a fraction of total liquid consumed) was calculated for each animal at each concentration. Tastants that are primarily salty (NaCl), sour (HCl), bitter (denatonium benzoate and quinine sulphate) or sweet (sucrose and the highly potent guanidine sweetener SC45647) to humans were tested. Two-factor (strain × concentration) analyses of variance (ANOVAs) (Table 1) were used to determine whether wild-type and null mice differed in their behavioural responses to tastants.

Responses of null mice to a concentration series of NaCl were similar to those of wild-type mice. Likewise, no strain difference was evident in the responses to a range of HCl solutions (Table 1; Fig. 2*a*, *b*). In both cases, all mice were indifferent to initial (low) tastant concentrations and exhibited aversive responses to higher concentrations. These data demonstrate that salty and sour behavioural responses are unaffected by the absence of α-gustducin.

In contrast, aversive responses to two bitter substances, denatonium benzoate and quinine sulphate, were diminished in the null mice compared to wild-type siblings (Table 1: Fig. 2*c*, *d*). Wild-type mice began to avoid denatonium at the 100 μM concentration, whereas null mice remained indifferent to denatonium even at 1 mM. The null mice required a ~40-fold higher concentration of denatonium and a ~100-fold higher concentration of